RESEARCH

Development of a prognostic surgical index using optical coherence tomography for large macular holes: a retrospective multicenter study

Yanting Li[1], Bin Chen[2], Xinzhu Chen[2] and Yunfeng Lu[1*]

Abstract

Background Herein, we developed a new index called the drawbridge index to predict surgical outcomes and assessed its value in guiding surgical decision-making for large macular holes (MHs) with diameters of 400–550 μm.

Methods A total of 48 eyes with large MHs (diameters of 400 to 550 μm), which had undergone vitrectomy with internal limiting membrane (ILM) peeling, were included and retrospectively analyzed. Based on optical coherence tomography images, base diameter, minimum linear diameter, the macular hole index (MHI), diameter hole index (DHI), and traction hole index (THI) were measured and calculated. The drawbridge index was calculated using the software ImageJ. It was determined by calculating the sum of the arm lengths extending from the break point of the outer plexiform layer (OPL) to the retinal pigment epithelium (RPE) on both sides of the macular hole, as well as the sum of the lengths from the starting point of the distorted OPL to the RPE in the vertical direction, and the difference between them then dividing by base diameter. The effectiveness of these predictive indices in prognosing "closed" versus "not closed" outcomes, and their correlation with outcome indicators, including best-corrected visual acuity, central foveal thickness, and ellipsoid zone defect length, was assessed. Furthermore, the area under the receiver operating characteristic curve (AUC) and a cutoff value were calculated for the drawbridge index. In the second part, a total of 21 patients were enrolled in the validation group, and the drawbridge index was utilized to guide surgical decisions for the ILM techniques.

Results Significant differences were observed between the "closed" and "not closed" groups using the drawbridge index ($P < 0.05$). The drawbridge index was significantly correlated with postoperative best-corrected visual acuity, ellipsoid zone defect, and central foveal thickness. It exhibited an AUC value of 0.92, and the cutoff value of 1.03 demonstrated a sensitivity of 87.50% and a specificity of 80.00%. Assisted by the drawbridge index, a 100% closure rate was achieved in patients in the validation group.

Conclusion The drawbridge index may be reliable and useful for making surgical decisions regarding ILM manipulation for large MHs.

*Correspondence:
Yunfeng Lu
luyunfeng99@yahoo.com
Full list of author information is available at the end of the article

Li *et al. BMC Ophthalmology*   (2025) 25:179

Page 2 of 8

Background

An idiopathic full-thickness macular hole (FTMH) is a retinal condition characterized by the complete absence of the retina at the fovea [1]. It can result in distorted vision and central scotoma, significantly compromising visual function. In terms of assessment, optical coherence tomography (OCT) is a valuable technique for visualizing the intricate structure of the retina and its ability to facilitate diagnosis and classify FTMHs [2].

FTMH can be effectively treated with pars plana vitrectomy (PPV), which incorporates either internal limiting membrane (ILM) peeling or ILM flap surgeries. Notably, ILM peeling techniques demonstrate a high closure rate of approximately 84–94% [3]. However, the closure rates are significantly low for large macular holes (MHs) with diameters greater than 400 μm. In these cases, ILM flap techniques are considered more effective in improving both anatomical and functional outcomes [4, 5]. A recent surgical classification of large FTMHs suggests that large MHs with diameters of 400–550 μm can be effectively treated with ILM peeling, whereas extra-large MHs with diameters of 550–800 μm require ILM flap techniques [6]. Therefore, the surgical approach for managing MHs with diameters of 400–550 μm remains controversial.

The purpose of the present study was to develop a novel index, the drawbridge index, to guide treatment decisions for MHs with diameters of 400–550 μm. The retrospective part of this study aimed to assess the effectiveness of the drawbridge index in predicting surgical results when using ILM peeling for MHs. The subsequent validation part aimed to confirm the utility of this index.

Methods

This study was conducted at two medical centers: (1) the first Affiliated Hospital of Soochow University and (2) Suzhou EENT Hospital. Approvals were obtained from the Institutional Review Boards of the First Affiliated Hospital of Soochow University and Suzhou EENT Hospital. This study adhered to the principles of the Declaration of Helsinki. In the retrospective part of the study, informed consent was waived owing to the retrospective nature of the study by the ethics committees of the First Affiliated Hospital of Soochow University and Suzhou EENT Hospital. Meanwhile, for the validation segment, informed consents were obtained from all participating patients.

Participants

Patients with large idiopathic FTMHs who underwent PPV combined with ILM peeling between January 2021 and December 2023 were retrospectively enrolled. In the validation part, patients diagnosed with idiopathic FTMHs between January 2024 and May 2024 underwent PPV based on the drawbridge index to determine the ILM technique and validate the index.

The inclusion criteria were as follows: (1) diagnosis of idiopathic FTMHs without other ocular diseases, except cataracts; (2) no previous optical surgery; (3) axial length between 21 mm and 26 mm, and myopia below – 6.00 diopters; and (4) FTMHs with minimum linear diameters in the range of 400 and 550 μm, as measured using the built-in OCT tool (the measurement method is described below).

Surgical treatment

All surgical procedures were performed by an experienced vitreoretinal surgeon. PPV was combined with phacoemulsification and intraocular lens implantation in eyes with cataracts. The standard three-port PPV procedure (Constellation; Alcon, Fort Worth, TX, USA) with complete posterior vitreous detachment (PVD) was performed. Indocyanine green dye was used to stain the ILM. In the ILM peeling technique, the stained ILM was delicately grasped with intraocular forceps (Revolution or Sharkskin; Alcon) and carefully peeled circularly within the vascular arcade, approximately 2 DD in diameter. Fluid-air exchange was performed at the end of the surgeries with air tamponade. Patients were advised to maintain a face-down position for 1 week.

Main measurements

The medical records included a comprehensive medical history and detailed ophthalmological examination, both preoperatively and approximately 1 month postoperatively. Axial lengths were measured, and intraocular lens calculations were performed before surgery using an optical measuring instrument (IOL-Master 500; Zeiss, Oberkochen, Germany; or Lenstar 900: Haag-Streit, Bern, Switzerland). Microstructural imaging of the macular fovea was performed using OCT (Optovue Inc., Fremont, CA, USA) preoperatively and 1 month postoperatively.

OCT examinations were conducted in the radial mode with 15-layer images (Fig. 1A). The built-in measurement tools of the OCT machines were employed to measure the minimum linear diameter (MLD), which was regarded as a critical index. Based on the result, the images with the largest MLD were selected as preoperative images for additional measurements, including the base diameter (BASE) and height of the macular
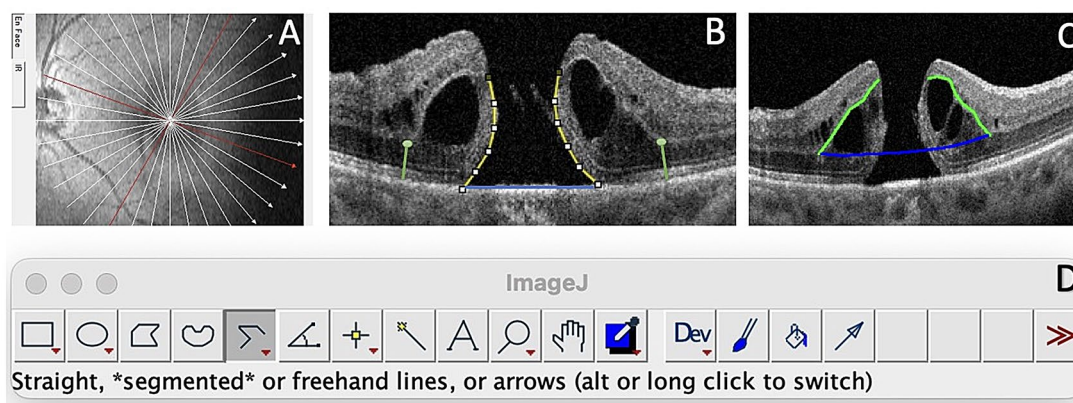
Fig. 1 The drawbridge index. (**A**) Optical coherence tomography examinations conducted in the radial mode with 15-layer images. (**B**) The drawbridge index is calculated using the following formula: (A-B) / **C**, where **A** is defined as the sum of the arm lengths extending from the break point of the outer plexiform layers to the retinal pigment epithelium on both sides of the macular hole (the sum of the lengths of the yellow curves); **B** is the sum of the lengths from the starting point of the outer plexiform layer (green points) to the retinal pigment epithelium in a vertical direction (the sum of the lengths of the green straight lines); and **C** is the length of the base diameter (the length of the blue straight line). (**C**) The probability of MH closure is associated with the combined length of the distorted outer plexiform layer on both sides of the macula (green lines), surpassing the total length of the MH lesion (blue line). (**D**) The "segment mode" of the Image J software is used for the measurement

hole (H). The predictive indices were calculated as follows: the macular hole index (MHI) [7] was calculated as MHI = H / BASE, H; the diameter hole index (DHI) [1] as DHI = MLD / BASE; and the traction hole index (THI) [1] as THI = H / MLD.

The drawbridge index was calculated using ImageJ software (version 1.53 K; National Institute of Health, Bethesda, MD, USA) with the "segment line" mode (Fig. 1D). It was defined as (A-B) / C (Fig. 1B), with "A" representing the sum of the arm lengths extending from the breakpoint of the outer plexiform layer (OPL) to the retinal pigment epithelium (RPE) on both sides of the macular hole (Fig. 1B, yellow segment curve lines), measured through six points along the profile to ensure accuracy; "B" indicating the sum of the lengths from the starting point of the distorted OPL (Fig. 1B, green points) to the RPE in the vertical direction (Fig. 1B, green straight lines); and "C" representing the base diameter (Fig. 1B, blue lines). The drawbridge index was developed based on that macular hole would possibly close when the combined length of the distorted OPL on both sides (Fig. 1C, green lines) exceeded the total length of the lesion (Fig. 1C, blue line), and it was designed to facilitate clinical application and reflect morphological characteristics within a specific MLD range.

One month postoperatively, OCT images displaying the poorest closure status in the radial mode were selected for categorization. Images showing the RPE exposed to the vitreous body were defined as "not closed" (group 1), while others were considered "closed" (group 2). The lengths of the ellipsoid zone (EZ) defects were confirmed, and a built-in tool was used to measure the defect and thickness of the central fovea (Additional File 1).

Two researchers calculated the indices using Microsoft software (Word and Excel for Mac, version 16.74; Microsoft Corp., Redmond, WA, USA). They worked independently and were blinded to the study content. All the measurements were repeated three times, and the intraclass correlation coefficient (ICC) was calculated. During the procedure, any discrepancies were addressed through discussion and re-measurements to ensure the accuracy of the results.

Statistical analyses

Data were analyzed using SPSS software (SPSS Inc., Chicago, IL, USA). Statistical comparisons of quantitative and categorical variables were conducted using the Mann–Whitney U test and chi-square test, respectively. For predictive and outcome indicators, Spearman's correlation coefficient test was used to examine correlations. Statistical significance was set at $P < 0.05$. Receiver operating characteristic (ROC) curves were used to assess predictive ability. The area under the ROC curve (AUC) was calculated. Cutoff values, determined as the maximum value of the Youden index (Youden's index = Sensitivity + Specificity – 1), were determined for the validation group, and ICC > 0.85 was considered reliable.

Results

Retrospective study

The retrospective study included 48 eyes with large FTMHs, including 18 eyes from men and 30 eyes from women. There were 4 patients with bilateral MHs. Among them, 1 patient had both eyes included in the retrospective study and 3 patients had only one eye included in the study, as the other eye did not meet the inclusion criteria. The demographic and baseline characteristics

Li *et al. BMC Ophthalmology*   (2025) 25:179

Page 4 of 8

Table 1 Demographic and baseline characteristics

N	48
Eye (L/R)	19/29
Sex (F/M)	30/18
pre BCVA (logMar)	1.11 ± 0.35
AL (mm, mean ± SD)	23.85 ± 0.35
Stage (3/4)	19/29
Age (years, mean ± SD)	64.83 ± 8.24
MLD (μm, mean ± SD)	493.10 ± 45.45
BD (μm, mean ± SD)	1060.00 ± 121.80
H (mean ± SD)	445.50 ± 80.50
MHI (mean ± SD)	0.42 ± 0.31
DHI (mean ± SD)	0.46 ± 0.06
THI (mean ± SD)	0.91 ± 0.19
Drawbridge index (mean ± SD)	1.25 ± 0.31

pre BCVA, preoperative best-corrected visual acuity; AL, axial length; Stage, Gass classification; MLD, minimum linear diameter; BD, base diameter; MHI, macular hole index; DHI, diameter hole index; THI, traction hole index

Table 2 Differences in characteristics and indices between the two groups

Group	Group 1	Group 2	*P*-value
N	8	40	-
Eye (L/R)	4/4	15/25	0.51
Sex (F/M)	4/4	26/14	0.42
Pre BCVA (logMar)	1.12 ± 0.02	1.11 ± 0.38	0.55
AL (mm, mean ± SD)	23.75 ± 0.79	23.87 ± 0.86	0.61
Stage (3/4)	2/6	17/23	0.35
Age (years, mean ± SD)	67.25 ± 5.15	64.35 ± 8.70	0.59
MLD (μm, mean ± SD)	520.40 ± 42.24	487.70 ± 44.57	0.06
BD (μm, mean ± SD)	1101.00 ± 213.30	1052.00 ± 96.50	0.30
H (mean ± SD)	431.90 ± 102.10	448.20 ± 76.76	0.77
MHI (mean ± SD)	0.40 ± 0.13	0.43 ± 0.07	0.26
DHI (mean ± SD)	0.48 ± 0.07	0.46 ± 0.06	0.86
THI (mean ± SD)	0.84 ± 0.25	0.92 ± 0.18	0.26
Drawbridge index (mean ± SD)	0.88 ± 0.11	1.32 ± 0.29	< 0.05

Statistical variables were analyzed using the Mann–Whitney U test, and categorical variables were analyzed using the chi-square test. Pre BCVA, preoperative best-corrected visual acuity; AL, axial length; Stage, Gass classification; MLD, minimum linear diameter; BD, base diameter; H, height; MHI, macular hole index; DHI, diameter hole index; THI, traction hole index

are summarized in Table 1. The MLD was 400–450 μm for 16 eyes, 450–500 μm for 16 eyes, and 500–550 μm for 16 eyes.

A total of 8 eyes that did not achieve closure were included in group 1, and 40 eyes that achieved closure were classified as group 2. The demographic and baseline characteristics of these groups are summarized in Table 2.

The age of groups 1 and 2 was 67.25 ± 5.15 years and 64.35 ± 8.70 years, respectively. Axial length in groups 1 and 2 was 23.75 ± 0.79 mm and 23.87 ± 0.86 mm, respectively. The preoperative best-corrected visual acuity (BCVA) in groups 1 and 2 was 1.12 ± 0.02 and 1.11 ± 0.38, respectively. According to the Gass classification at baseline in group 1, stage 3 was present in 2 eyes and stage 4 in 6 eyes. In group 2, stage 3 was present in 17 eyes and stage 4 in 23 eyes. There were no significant differences between the two groups regarding age ($P = 0.59$), axial length ($P = 0.61$), preoperative BCVA ($P = 0.55$), or sex ($P = 0.42$). Additionally, no differences were observed in indices of MLD ($P = 0.06$), BD ($P = 0.30$), H ($P = 0.77$), MHI ($P = 0.26$), DHI ($P = 0.86$), and THI ($P = 0.26$). Significant differences were observed in the drawbridge index ($P < 0.05$).

In Spearman's correlation analysis, BD was significantly correlated with postoperative BCVA ($r = 0.26$, $P < 0.05$), EZ defects ($r = 0.20$, $P < 0.05$), and CFT ($r = -0.28$, $P < 0.05$). MHI was significantly correlated with postoperative BCVA ($r = -0.25$, $P < 0.05$) and CFT ($r = 0.33$, $P < 0.05$). THI was significantly correlated with CFT ($r = 0.25$, $P < 0.05$). MLD and DHI were not significantly correlated with the result parameters. Notably, the drawbridge index was significantly correlated with postoperative BCVA, EZ defect, and CFT (Table 3).

In addition, the ROC curve was plotted, and the AUC was calculated. The AUC of drawbridge index was 0.92, illustrating its effectiveness. The cutoff value of the drawbridge index was 1.03, with a sensitivity of 87.50% and a specificity of 80.00%.

Table 3 Spearman's correlation coefficients for the correlations between predictive indices and outcome indicators

	Post BCVA		EZ defect		CFT	
	P	r	P	r	P	r
MLD	0.11	0.18	0.19	0.12	0.12	-0.17
BD	< 0.05	0.26	< 0.05	0.20	< 0.05	-0.28
Drawbridge index	< 0.05	-0.67	< 0.05	-0.70	< 0.05	0.56
H	0.30	-0.07	0.43	-0.02	0.15	0.16
MHI	< 0.05	-0.25	0.08	-0.20	< 0.05	0.33
DHI	0.34	-0.05	0.10	-0.19	0.33	0.06
THI	0.15	-0.15	0.27	-0.09	< 0.05	0.25

Post BCVA, postoperative best-corrected visual acuity; EZ, ellipsoid zone; CFT, central foveal thickness; MLD, minimum linear diameter; BD, base diameter; MHI, macular hole index; DHI, diameter hole index; THI, traction hole index

Li *et al. BMC Ophthalmology*   (2025) 25:179

Page 5 of 8

Validation study

A total of 21 patients were enrolled in the validation group, and the drawbridge index was used to guide surgical decisions. No significant differences were observed in basic characteristics, including age, sex, and BCVA (Table 4). A threshold value of 1.03 was established, and values above the threshold indicated a preference for the ILM peeling method, whereas values below the threshold suggested the potential need for an inverted ILM approach. All patients achieved success at 1 month postoperatively.

Discussion

The PPV technique, initially introduced by Kelly and Wendel in 1991, has become the gold standard surgical treatment for idiopathic FTMH [8]. ILM peeling is a crucial surgical step to alleviate tangential traction forces around the fovea and ensure complete removal of epiretinal tissue [9, 10]. ILM flap techniques are recommended for large MHs with diameters larger than 400 μm [11]. Recent updates in the surgical classification of large MHs suggest that the ILM flap technique should be employed for MHs with MLDs > 550 μm [6]. The Manchester Large Macular Hole Study suggested that MLD > 650 μm necessitates the ILM flap method [12]. While the ILM flap technique offers advantages such as a scaffold for the proliferation and migration of Müller cells [13], it may result in complications such as macular pucker and excessive gliosis [14]. Moreover, the technique is time-consuming and requires great skill to ensure that the flap attaches [15]. Ventre et al. [16] have concluded that better functional outcomes in macular sensitivity could be achieved with ILM peeling than with the inverted flap technique for small-to-medium MHs. Therefore, the definitive surgical choice for MHs sized between 400 and 550 μm, traditionally classified as large MHs, remains worthy of further discussion.

Thus, in the present study, we introduced the drawbridge index, inspired by the hydration theory [17], which first used the "drawbridge" metaphor according to

OCT images. These images enabled visualization of the detailed structure of an MH, whether open or closed. As the MH forms, the accumulation of cystoid spaces within the foveal walls, between the OPL and Henle fiber layer, leads to the enlargement of the MH [18], creating a "pregnant drawbridge" appearance. As the traction resolves and the cystoid spaces are absorbed, the MH gradually closes, as does the drawbridge.

Theoretically, the annular contraction of the parafoveal Müller cell side processes in the OPL is a critical factor in the early closure of MHs, followed by a centripetal shift and restructuring of central photoreceptors [19, 20]. Clinically, irrespective of whether the MH closure resulted from surgical intervention or occurred spontaneously, we observed the initial connections occurring at the OPL level (Fig. 2). Based on this, we hypothesized that the probability of MH closure was associated with the combined length of the distorted OPL on both sides of the macula, surpassing the total length of the MH lesion (Fig. 1C). The threshold value should theoretically be 1, indicating the fusion of Müller cell structure remnants at the OPL level [21]. This process is akin to a drawbridge, where if the planks on both sides align with the total length of the bridge, it can fully close. However, in practice, direct measurement of the OPL may be impractical, owing to potential deformations in the OCT images. Therefore, the drawbridge index is calculated by summing the arm lengths from the point of break in the OPL to the RPE and subtracting the sum of the lengths from the OPL to the RPE vertically. When this length equals to the diameter in OPL level of macular hole, closure of the drawbridge becomes possible. To facilitate measurement and enhance closure efficiency, we used the base diameter, which was slightly larger than the length of the OPL level. This may explain why the drawbridge index yielded better visual results and performed well in the validation group. Although this index is not precise, it remains a useful tool. Moreover, the ROC curve highlighted the notable diagnostic performance of this index, with an AUC value of 0.92 and a cutoff value of 1.03, aligning with our hypothesis.

In the validation part of the study, an index score below the cutoff value of 1.03 suggested potential insufficient closure, indicating that the inverted ILM flap technique was needed, even if the diameter was below 550 μm. ILM peeling was recommended when the index was above 1.03. In the validation group, we achieved a 100% closure rate using the new index.

Roth et al. conducted a comprehensive evaluation of commonly used clinical and OCT morphological prognostic parameters for postoperative outcomes following MH surgery and concluded that MLD is a robust prognostic factor [22]. However, our results suggested that the MLD may not always be a critical factor in some

Table 4 Demographic and baseline characteristics of the observational and validation groups

	Observational group	Validation group	*P*
N	48	21	-
Eye (L/R)	19/29	11/10	0.32
Sex (F/M)	30/18	14/7	0.74
pre BCVA (logMar)	1.11±0.35	1.03±0.31	0.77
AL (mm, mean±SD)	23.85±0.35	23.32±0.60	0.57
Stage (3/4)	19/29	8/13	0.90
Age (years, mean±SD)	64.83±8.24	66.52±5.80	0.78
MLD (μm, mean±SD)	493.10±45.45	504.62±40.49	0.35

pre BCVA, preoperative best-corrected visual acuity; AL, axial length; Stage, Gass classification; MLD, minimum linear diameter
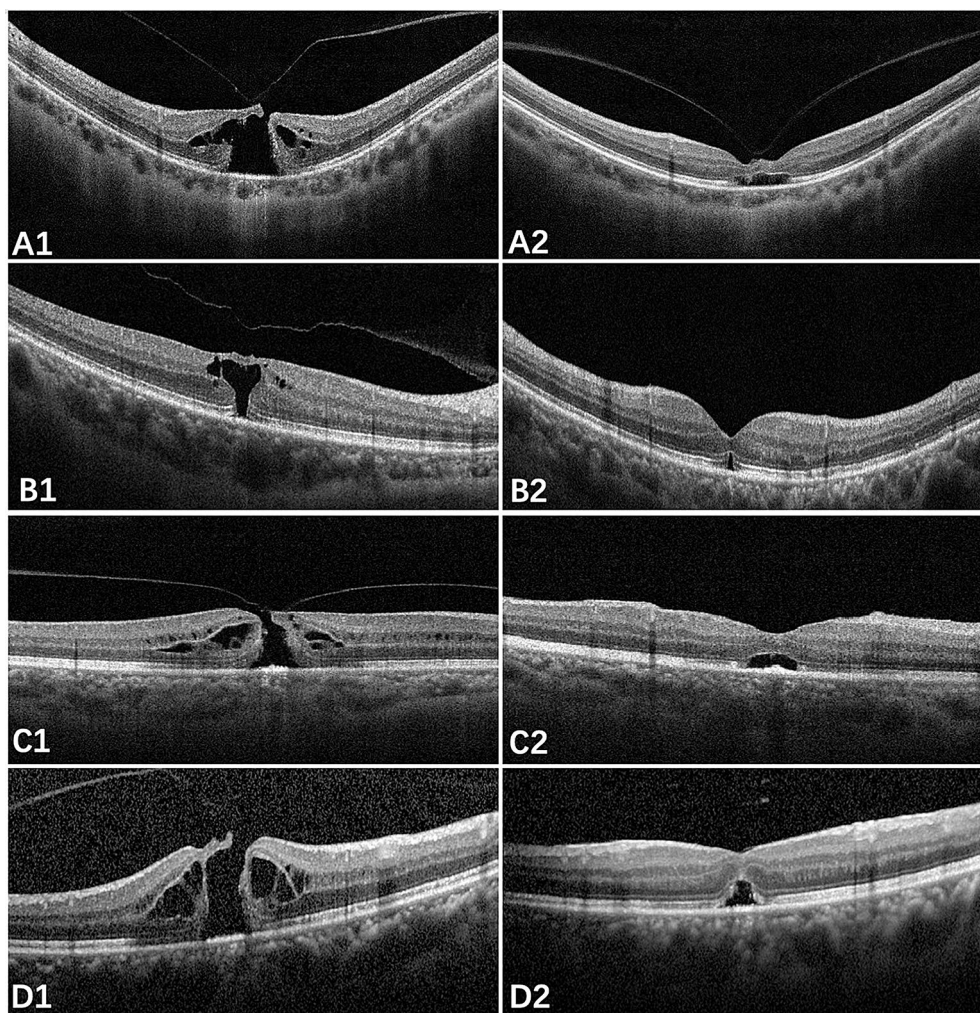
Fig. 2 Closure of the macular holes. The optical coherence tomography images depicted in **A1** and **B1** are two macular holes, which have spontaneously closed. Their early closures are presented in **A2** and **B2**, demonstrating the connections of macular holes at the outer plexiform layer level. The optical coherence tomography images depicted in **C1** and **D1** are two macular holes, which have closed after ILM peeling surgeries. The early stage of closure is depicted in **C2** and **D2**, illustrating the connections of macular holes at the outer plexiform layer level

conditions. In the retrospective part of our study, within a specific MLD range no significant differences were observed among the MLD, MHI, DHI, and THI between the closure and non-closure groups. This finding suggests that MHs with diameters of a certain range may share similar characteristics, making the MHI, DHI, and THI, which were previously considered useful indices [1, 7], ineffective in predicting closure outcome although they still correlated with visual outcomes. Instead, the drawbridge index accounted for variations in intraretinal edema and base diameter, as different levels of edema could be accessed through the arm lengths from the OPL to the RPE. This approach emphasizes the morphology of macular hole, which is crucial for understanding the underlying causes and key factors contributing to surgical failure.

This study had some limitations. First, the accuracy of the calculation process depended on the skill level of the researcher and image quality; this limitation may be addressed through advancements in OCT machines, along with the assistance of software tools. Second, 2D imaging has inherent limitations, as different layers and modes can yield varying results. For instance, the image with the largest MLD may not necessarily correspond to the one with the greatest BD or height. In the future, a 3D-based drawbridge index could offer a promising direction. Third, we primarily focused on the early stages of MH closure. It is important to note that the initiation of foveal shape regeneration typically begins about 1 month after hole closure and spans 1.5 months [23]. Therefore, a long-term study is necessary, and we plan to conduct a randomized trial with a control group

Li *et al. BMC Ophthalmology*   (2025) 25:179

Page 7 of 8

to facilitate a comprehensive comparison, ultimately enhancing the scientific rigor and reliability of the results.

Conclusions

In conclusion, the drawbridge index is grounded in anatomical foundations and based on OCT images. Through this study, we demonstrated the effective predictive ability of the index, providing valuable guidance for making surgical decisions regarding ILM management of large MHs with diameters ranging from 400 to 550 µm. Further research should aim to assess the accuracy and feasibility of the drawbridge index for predicting foveal structure and long-term visual outcomes.

Abbreviations
AUC	Area Under the Receiver Operating Characteristic Curve
BASE	Base Diameter
CFT	Central Foveal Thickness
DHI	Diameter Hole Index
EZ	Ellipsoid Zone
FTMH	Full-Thickness Macular Hole
H	Height of the Macular Hole
ILM	Inner Limiting Membrane
MHI	Macular Hole Index
MHs	Macular Holes
MLD	Minimum Linear Diameter
OCT	Optical Coherence Tomography
OPL	Outer Plexiform Layer
PPV	Pars Plana Vitrectomy
PVD	Posterior Vitreous Detachment
ROC	Receiver Operating Characteristic
RPE	Retinal Pigment Epithelium
THI	Traction Hole Index

Supplementary Information

The online version contains supplementary material available at https://doi.org/10.1186/s12886-025-03998-w.

Supplementary Material 1: Postoperative optical coherence tomography (OCT) images. (A) Complete closure; (B) closure with subretinal fluid; (C) unclosed macular hole; (D) poor closure of macular hole with EZ distortion (red arrow). Description of data: This file contains postoperative OCT images showing various outcomes of the surgical procedure. Panel A illustrates complete closure of the macular hole, Panel B shows closure with subretinal fluid, Panel C depicts an unclosed macular hole, and Panel D presents a case of poor closure with distortion of the ellipsoid zone (EZ), indicated by a red arrow.

Author contributions
All authors contributed to the study conception and design. Material preparation, data collection and analysis were performed by Yanting Li, Bin Chen, Xinzhu Chen. The first draft of the manuscript was written by Yanting Li and Yunfeng Lu. All authors commented on previous versions of the manuscript. All authors read and approved the final manuscript.

Data availability
The datasets generated and/or analysed during the current study are not publicly available due to an ongoing study with the same group of patients but are available from the corresponding author on reasonable request.

Declarations

Ethics approval and consent to participate
Approval was obtained from the Institutional Review Boards of Suzhou University Affiliated First Hospital (No. 2024−459) and Suzhou EENT Hospital (No. 2024-08). This study adhered to the principles of the Declaration of Helsinki. In the retrospective part of the study, informed consent was waived due to the study's nature by the ethics committees of the First Affiliated Hospital of Soochow University and Suzhou EENT Hospital. However, for the verified segment, informed consent was obtained from all participating patients.

Consent for publication
Not applicable.

Competing interests
The authors declare no competing interests.

Author details
[1]Department of Ophthalmology, The First Affiliated Hospital of Soochow University, Shizi Street 188, Suzhou, Jiangsu Province 215000, China
[2]Department of Ophthalmology, Suzhou EENT Hospital, Suzhou, Jiangsu Province 215000, China

References
1. Ruiz-Moreno JM, Staicu C, Piñero DP, Montero J, Lugo F, Amat P. Optical coherence tomography predictive factors for macular hole surgery outcome. Br J Ophthalmol. 2008;92:640–4. https://doi.org/10.1136/bjo.2007.136176.
2. Ittarat M, Somkijrungroj T, Chansangpetch S, Pongsachareonnont P. Literature review of surgical treatment in idiopathic full-thickness macular hole. Clin Ophthalmol. 2020;14:2171–83. https://doi.org/10.2147/OPTH.S262877.
3. Andrew N, Chan WO, Tan M, Ebneter A, Gilhotra JS. Modification of the inverted internal limiting membrane flap technique for the treatment of chronic and large macular holes. Retina. 2016;36:834–7. https://doi.org/10.1097/IAE.0000000000000931.
4. Michalewska Z, Michalewski J, Adelman RA, Nawrocki J. Inverted internal limiting membrane flap technique for large macular holes. Ophthalmology. 2010;117:2018–25. https://doi.org/10.1016/j.ophtha.2010.02.011.
5. Velez-Montoya R, Ramirez-Estudillo JA, Sjoholm-Gomez de Liano C, Bejar-Cornejo F, Sanchez-Ramos J, Guerrero-Naranjo JL, et al. Inverted ILM flap, free ILM flap and conventional ILM peeling for large macular holes. Int J Retina Vitreous. 2018;4:8. https://doi.org/10.1186/s40942-018-0111-5.
6. Rezende FA, Ferreira BG, Rampakakis E, Steel DH, Koss MJ, Nawrocka ZA, et al. Surgical classification for large macular hole: based on different surgical techniques results: the CLOSE study group. Int J Retina Vitreous. 2023;9:4. https://doi.org/10.1186/s40942-022-00439-4.
7. Kusuhara S, Teraoka Escaño MF, Fujii S, Nakanishi Y, Tamura Y, Nagai A, et al. Prediction of postoperative visual outcome based on hole configuration by optical coherence tomography in eyes with idiopathic macular holes. Am J Ophthalmol. 2004;138:709–16. https://doi.org/10.1016/j.ajo.2004.04.063.
8. Kelly NE, Wendel RT. Vitreous surgery for idiopathic macular holes. Results of a pilot study. Arch Ophthalmol. 1991;109:654–9. https://doi.org/10.1001/archopht.1991.01080050068031.
9. Morizane Y, Shiraga F, Kimura S, Hosokawa M, Shiode Y, Kawata T, et al. Autologous transplantation of the internal limiting membrane for refractory macular holes. Am J Ophthalmol. 2014;157:861–e91. https://doi.org/10.1016/j.ajo.2013.12.028.
10. Lois N, Burr J, Norrie J, Vale L, Cook J, McDonald A, et al. Internal limiting membrane peeling versus no peeling for idiopathic full-thickness macular hole: a pragmatic randomized controlled trial. Invest Ophthalmol Vis Sci. 2011;52:1586–92. https://doi.org/10.1167/iovs.10-6287.
11. Duker JS, Kaiser PK, Binder S, de Smet MD, Gaudric A, Reichel E, et al. The international vitreomacular traction study group classification of vitreomacular adhesion, traction, and macular hole. Ophthalmology. 2013;120:2611–9. https://doi.org/10.1016/j.ophtha.2013.07.042.
12. Ch'ng SW, Patton N, Ahmed M, Ivanova T, Baumann C, Charles S, et al. The Manchester large macular hole study: is it time to reclassify large macular

holes? Am J Ophthalmol. 2018;195:36–42. https://doi.org/10.1016/j.ajo.2018.07.027.

13. Shiode Y, Morizane Y, Matoba R, Hirano M, Doi S, Toshima S, et al. The role of inverted internal limiting membrane flap in macular hole closure. Invest Ophthalmol Vis Sci. 2017;58:48470–55. https://doi.org/10.1167/iovs.17-21756.

14. Kanda K, Nakashima H, Emi K. Macular pucker formation after inverted internal limiting membrane flap technique: two case reports. Am J Ophthalmol Case Rep. 2022;25:101282. https://doi.org/10.1016/j.ajoc.2022.101282.

15. Yang JM, Kim JG. Internal limiting membrane handling in macular hole surgery: the infusion direction manipulation and infusion off techniques. Eur Rev Med Pharmacol Sci. 2022;26:2395–8. https://doi.org/10.26355/eurrev_202204_28471.

16. Ventre L, Fallico M, Longo A, Parisi G, Russo A, Bonfiglio V, et al. Conventional internal limiting membrane peeling versus inverted flap for small-to-medium idiopathic molecular hole: a randomized trial. Retina. 2022;42:2251–7. https://doi.org/10.1097/IAE.0000000000003622.

17. Tornambe PE. Macular hole genesis: the hydration theory. Retina. 2003;23:421–4. https://doi.org/10.1097/00006982-200306000-00028.

18. Bringmann A, Unterlauft JD, Barth T, Wiedemann R, Rehak M, Wiedemann P. Müller cells and astrocytes in tractional macular disorders. Prog Retin Eye Res. 2022;86:100977. https://doi.org/10.1016/j.preteyeres.2021.100977.

19. Bringmann A, Duncker T, Jochmann C, Barth T, Duncker GIW, Wiedemann P. Spontaneous closure of small full-thickness macular holes: presumed role of Müller cells. Acta Ophthalmol. 2020;98:e447–56. https://doi.org/10.1111/aos.14289.

20. Reichenbach A, Bringmann A. Glia of the human retina. Glia. 2020;68:768–96. https://doi.org/10.1002/glia.23727.

21. Gupta B, Laidlaw DA, Williamson TH, Shah SP, Wong R, Wren S. Predicting visual success in macular hole surgery. Br J Ophthalmol. 2009;93:1488–91. https://doi.org/10.1136/bjo.2008.153189.

22. Roth M, Schön N, Jürgens L, Engineer D, Kirchhoff K, Guthoff R, et al. Frequently assessed and used prognostic factors for outcome after macular hole surgery: which is better? BMC Ophthalmol. 2021;21:398. https://doi.org/10.1186/s12886-021-02164-2.

23. Govetto A, Hubschman JP, Sarraf D, Figueroa MS, Bottoni F, dell'Omo R, et al. The role of Müller cells in tractional macular disorders: an optical coherence tomography study and physical model of mechanical force transmission. Br J Ophthalmol. 2020;104:466–72. https://doi.org/10.1136/bjophthalmol-2019-314245.

Publisher's note